International Journal of Minerals, Metallurgy and Materials
Volume 24, Number 9, September 2017, Page 1010
DOI: 10.1007/s12613-017-1490-6

Effect of prolonged isothermal heat treatment on the mechanical behavior of advanced NANOBAIN steel

Behzad Avishan

Department of Materials Engineering, Azarbaijan Shahid Madani University, Tabriz 53714-161, Iran
(Received: 3 November 2016; revised: 4 April 2017; accepted: 5 April 2017)

Abstract: The microstructural evolution and consequent changes in strength and ductility of advanced NANOBAIN steel during prolonged isothermal heat-treatment stages were investigated. The microstructure and mechanical properties of nanostructured bainite were not expected to be influenced by extending the heat-treatment time beyond the optimum value because of the autotempering phenomenon and high tempering resistance. However, experimental results indicated that the microstructure was thermodynamically unstable and that prolonged austempering resulted in carbon depletion from high-carbon retained austenite and carbide precipitations. Therefore, austenite became thermally less stable and partially transformed into martensite during cooling to room temperature. Prolonged austempering did not lead to the typical tempering sequence of bainite, and the sizes of the microstructural constituents were independent of the extended heat-treatment times. This independence, in turn, resulted in almost constant ultimate tensile strength values. However, microstructural variations enhanced the yield strength and the hardness of the material at extended isothermal heat-treatment stages. Finally, although microstructural changes decreased the total elongation and impact toughness, considerable combinations of mechanical properties could still be achieved.

Keywords: nano bainite; steel; prolonged austempering; microstructure; mechanical properties

1. Introduction

The presence of carbide particles restricts the industrial applications of steels with upper and lower bainite morphologies, especially in applications that require steel with high toughness and high ductility. In this regard, the judicious use of silicon in the chemical composition inhibits carbide precipitation; therefore, carbon remains in solid solution within the austenite phase, which reduces its martensite start temperature and makes it stable at room temperature [1–3]. Therefore, the final microstructure will be carbide-free bainite with an acceptable balance of strength and ductility because of the replacement of brittle carbide with ductile austenite phase within the microstructure. A new group of carbide-free bainitic steels known as nanostructured-low temperature bainitic steels, or advanced NANOBAIN steels, has recently been introduced; according to current metallurgical phase transformation theories and thermodynamic facts, these steels can be attained through a simple isothermal heat treatment at temperatures less than 400°C [4–15]. The final microstructures are bainitic ferrites of 20–100 nm thick depending on the heat treatment temperature, separated by austenite films of almost identical sizes. Such a unique microstructure results in a superior ultimate tensile strength (UTS) of almost 2 GPa in combination with noticeable uniform elongation [16–17].

The thermodynamic theory of bainitic transformation has been discussed in detail elsewhere [18]. Bainite formation starts with paraequilibrium nucleation of ferrite plates and progresses via their shear growth [19]. Decreasing the transformation temperature increases the driving force of the bainite nucleation, which results in higher volume fractions of bainitic subunits. Similar to martensitic transformations, no alloying element redistributions occur during bainite formation, except for carbon, which partitions from ferrite to austenite because of the higher transformation temperatures of the bainitic reaction [20–21]. This behavior is similar to that at the first stage of martensite tempering and is known

Corresponding author: Behzad Avishan E-mail: avishan@azaruniv.ac.ir

as the autotempering phenomenon, which is an unavoidable part of the bainitic reaction [18]. However, the strain accommodation accompanied by the shear transformation mechanism of the bainitic transformation results in high dislocation densities, which are responsible for differences in the mechanical and physical properties of nanobainite obtained at different temperatures, which, in turn, affects the autotempering and extent of carbon depletion from ferrite to the surrounding austenite. Carbon atoms prefer to segregate to dislocations rather than precipitating because the segregation at dislocation cores results in a greater decrease of the free energy. This effect has been previously demonstrated in detailed atom probe tomography (APT) studies [22–24].

Bainitic transformation never goes to completion and stops when the carbon content of austenite reaches that predicted by the T□ diagram, which is the locus of the points at which ferrite and austenite with the same chemical composition have the same free energies. This effect is known as the incomplete transformation phenomenon and must be taken into account during bainitic transformation studies [22,25–26]. The time at which bainitic transformation stops is known as the optimum bainitic heat-treatment time, at the end of which the microstructure contains bainitic sheaves (alternating layers of bainitic subunits and carbide-free austenite films, both with nanoscale sizes) separated by carbide-free austenite microblocks [27]. To acquire the desired microstructural characteristics and optimum mechanical properties, care must be taken to conduct the bainitic heat treatment for optimum austempering times at each transformation temperature. However, the resulting microstructure appears to be thermodynamically unstable at the end of the optimum heat-treatment time because transformation stops before the austenite carbon content reaches that predicted by the Ae_3 curve; i.e., incomplete transformation occurs. Therefore, microstructural changes can presumably be introduced by extending the transformation time at the transformation temperature, similar to what happens during tempering at higher temperatures. Although the tempering of carbide-free bainite has been studied at ordinary high temperatures of 400–750°C, which are well above the transformation temperature of advanced bainite [28–31], understanding what happens if isothermal heat treatment is extended to heat-treatment times beyond the optimum time, even at transformation temperature ranges, is critical. This knowledge would highlight the importance of the optimum austempering time because any possible microstructural changes would directly affect the final comprehensive mechanical properties. In this regard, in this work, we investigate the variations of strength, ductility, and impact toughness at the end of the optimum and prolonged isothermal heat-treatment stages according to the microstructural evolutions.

2. Experimental procedures

Steel with a chemical composition of 0.88C–1.62Si–1Cr–0.27Mo–2.55Ni–1.20Mn–0.89Al–1.22Co–0.1V (wt%) was casted in an induction furnace, homogenized at 1200°C for 4 h, hot rolled into sheets of 15 mm thick, and finally ground to obtain parallel surfaces and to remove the decarburized layers. A large amount of carbon was essential to decrease the martensite and bainite start temperatures, enabling the formation of nanobainite at low temperatures. In addition, the addition of almost 1.6wt% silicon retarded the cementite precipitation, which made the carbon remain in the solid solution in austenite and made the austenite stable at room temperature. Cobalt and aluminum were also added to accelerate the transformation kinetics [32] because completion of the bainitic transformation at low transformation temperatures has been demonstrated to require several days [18]. Furthermore, the addition of molybdenum was required to prevent temper embrittlement due to phosphorus and the additions of manganese, chromium, and nickel were necessary to increase the hardenability. Finally vanadium was added for controlling the primary austenite grain size, which has been shown to detrimentally increase the potential nucleation sites of bainitic ferrites and subsequently increase the transformation rate [17,33].

After austenitization at 950°C for 30 min, advance bainite microstructures were obtained by isothermal austempering at three different temperatures of 300, 250, and 200°C for optimum heat-treatment times of approximately 10, 16, and 72 h, respectively. Both austenitizing and austempering heat treatments were conducted in salt-bath furnaces. To study the effect of prolonged heat treatment conditions on microstructural features and mechanical properties, two stages of prolonged isothermal heat treatments were designed. Test samples were heat treated for 20, 32, and 144 h in the first stage and for 30, 48, and 216 h in the second stage at each of the respective transformation temperature mentioned previously; thus, the heat-treatment times were two and three times longer, respectively, than the optimum times at the two stages. All samples were cooled to room temperature using 25°C water immediately after completion of the heat-treatment procedures.

Detailed microstructural evaluations were conducted using a Phenom ProX^{TM} scanning electron microscope after the samples were ground, polished, and etched using 2%

nital etchant solution according to the standard procedures. High-magnification scanning electron microscopy (SEM) micrographs were collected to measure the thicknesses of the bainitic subunits and austenite films using the line-intercept method [34]. Moreover, energy-dispersive X-ray (EDX) analysis was used in conjunction with SEM when needed. X-ray diffraction (XRD) analyses were conducted on a Bruker-Axs D8 Advance™ diffractometer with a Cu K_α radiation source operated at 40 kV and 40 mA. Scanning was performed at a rate of $0.02°\cdot min^{-1}$ in the 2θ range from 40° to 101°. XRD profile refinements were used to determine the volume fraction of high-carbon retained austenite using the integrated intensities of the (200), (220), and (311) peaks of austenite and the (200), (211), and (220) peaks of ferrite [35]. The XRD results were also used to determine the chemical composition of the retained austenite according to the well-known Dyson and Holmes' equation [36] based on the austenite lattice parameter determined using the Cohen's method [35,37]. The Dyson and Holmes' equation relates the austenite lattice parameter to its chemical composition; this method is applied by considering the paraequilibrium nucleation and shear growth mechanism of bainite, which means that only carbon diffuses during the bainite nucleation stage and that growth occurs without diffusion of any alloying elements.

Hardness values were measured on the HV30 scale using an Ease Way™ machine; the reported values are the average of at least five different measurements. Flat tensile test samples with a 9.8-mm gage length were cut and machined from primary sheets according to standard JISZ2201; the samples were isothermally heat treated for optimum and prolonged heat-treatment times. Tensile tests were performed on an Instron 8502™ testing machine assisted by an extensometer that enabled the continuous tracking of load–displacement data during the tests. Finally, charpy impact tests were conducted at room temperature with a standard Roell Amsler™ testing machine using notched samples of 10 mm × 10 mm × 55 mm austempered for optimum and prolonged heat-treatment times.

3. Results and discussion

3.1. Microstructural evaluations

Fig. 1 illustrates the microstructural characteristics of steel samples transformed to bainite under each heat-treatment condition. The results indicate that bainitic ferrites and high-carbon retained austenite were the only phases present within the microstructure. In addition, because of the appropriate chemical composition design and sufficiently high hardenability of the samples, preliminary evaluations failed to reveal any diffusional phase transformation products such as pearlite or ferrite at any stage of bainitic heat treatment. Furthermore, martensite transformation was inhibited by the high-carbon content of the bulk material and by additional carbon enrichment of austenite during the bainitic transformation. The SEM micrographs in Fig. 1 show that each sheaf contained parallel layers of dark bainitic subunits separated by light austenite films and that austenite microblocks separated the bainitic sheaves.

Quantitative measurements based on high-magnification SEM pictures are summarized in Table 1. These results confirm that we obtained nanostructured bainitic steels with nanoscale bainitic ferrites and austenite films, both approximately 41–88 nm thick, depending on the heat-treatment temperature and time. Given the optimum heat treatment conditions, decreasing the transformation temperature clearly resulted in refining the microstructure of bainite. Microstructural refinement is affected by the strength of primary austenite, the driving force of the transformation, and the transformation temperature, and these parameters are the most important parameters governing the size of the microstructural constituents [38]. A higher strength of the austenite phase at lower transformation temperatures constrains the motion of the glissile interface of ferrite and austenite, which ultimately results in thinner bainitic subunits at the end of the growth stage of ferrite plates. Moreover, a higher driving force of bainite nucleation at lower transformation temperatures results in more severe intersections of bainitic ferrites and therefore results in restriction of their growth, which means that finer subunits of bainite and, consequently, finer bainitic sheaves can be achieved at the end of the transformation. Notably, the sizes and the thicknesses of austenite films are affected by the thicknesses of the bainitic subunits; consequently, thinner films of austenite are expected if thinner bainitic subunits are achieved [34].

Quantitative data revealed no distinctive changes in the size of the microstructural constituents at the end of the first and second stages of prolonged heat-treatment procedures compared to that at the end of optimum austempering times. This similarity means that the sizes of the bainitic ferrites and austenite films are not sensitive to the extension of heat-treatment time at any of the heat-treatment temperature. Nevertheless, the changes in the volume fraction of retained austenite within the microstructure should be informative. Fig. 2 compares the volume fractions of high-carbon retained austenite being present within the microstructure at the end of the first and second stages of the prolonged isothermal heat treatment conditions, with that of obtained at

the end of optimum austempering times. As evident in Fig. 2, 38vol%, 28vol%, and 24vol% of high-carbon retained austenite were present within the microstructure when bainitic transformation was completed at 300, 250, and 200°C, respectively. However, the austenite contents decreased to approximately 34vol%, 22vol%, and 19vol% at the end of the first stage and to 33vol%, 20vol%, and 18vol% at the end of the second stage of the prolonged austempering heat treatments at each of the aforementioned transformation temperatures, respectively.

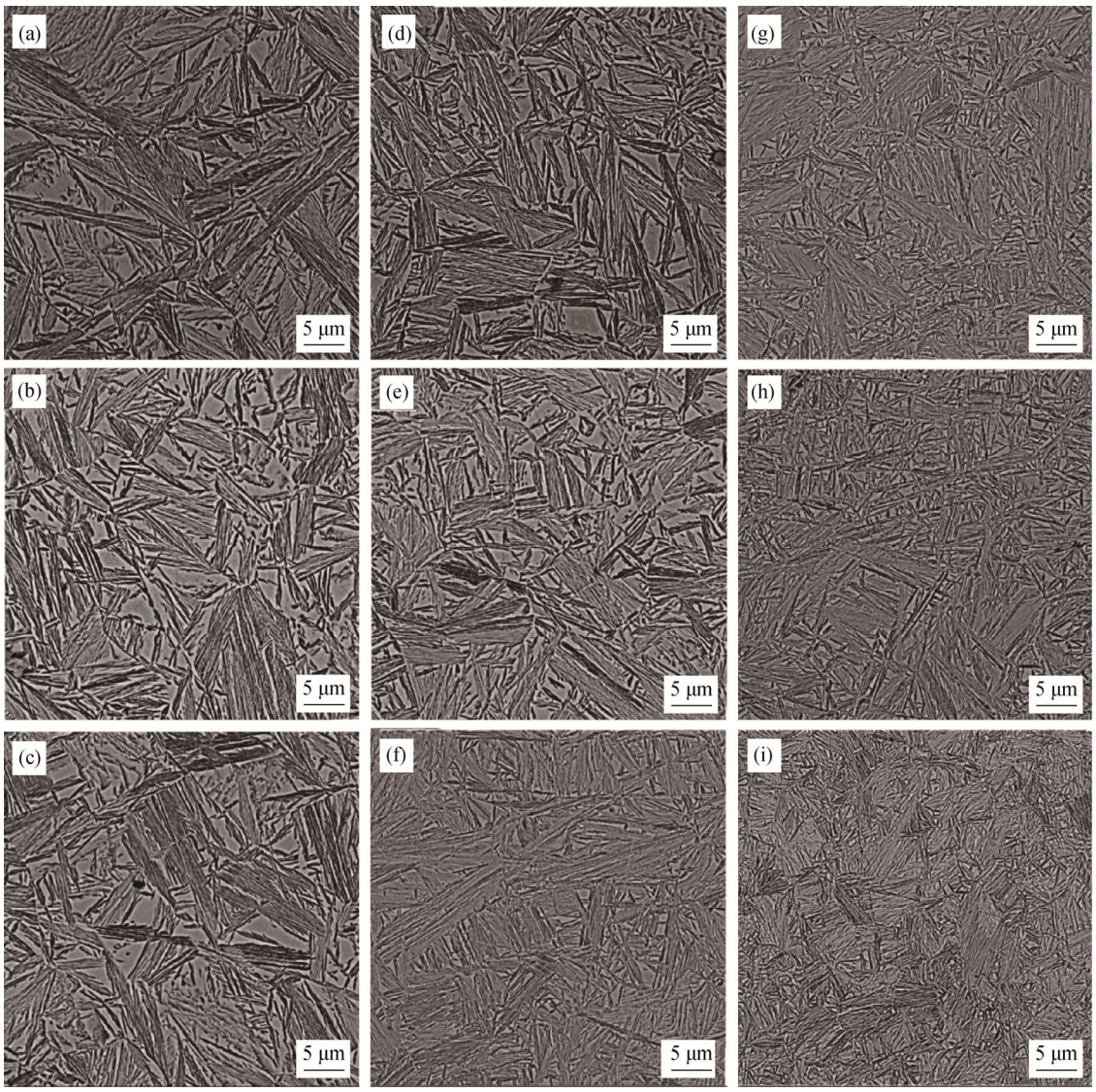

Fig. 1. SEM micrographs of advanced bainite formed under different conditions: (a) 300°C, 10 h; (b) 300°C, 20 h; (c) 300°C, 30 h; (d) 250°C, 16 h; (e) 250°C, 32 h; (f) 250°C, 48 h; (g) 200°C, 72 h; (h) 200°C, 144 h; (i) 200°C, 216 h.

Table 1. Thicknesses of bainitic subunits (t_α) and austenite films (t_γ) at different heat-treatment temperatures and times

Thickness / nm	300°C			250°C			200°C		
	10 h	20 h	30 h	16 h	32 h	48 h	72 h	144 h	216 h
t_α	78 ± 2	80 ± 2	77±3	66 ± 3	65 ± 3	66 ± 2	45 ± 3	47 ± 3	44 ± 1
t_γ	83 ± 2	85 ± 3	82±4	71 ± 3	74 ± 1	69 ± 3	60 ± 3	55 ± 3	54 ± 3

Such a trend can be rationalized on the basis of carbon content measurements at different stages of heat treatment. Table 2 shows the chemical composition of retained austenite calculated on the basis of its lattice parameter derived from XRD refinements and following the procedure described by Dyson and Holmes [36]. Other than the higher

carbon content, no distinctive differences were observed between the chemical compositions of retained austenite and the primary chemical composition of the bulk material at the end of the optimum heat-treatment time. This similarity in compositions can be rationalized by the facts that the bainitic transformation is diffusionless and that only carbon diffuses during the nucleation of bainitic ferrites, which means $(X_{Fe}/X_j)_{bulk} = (X_{Fe}/X_j)_{austenite}$, where j denotes any substitutional element in the alloy, and X_{Fe} and X_j are the concentrations of iron and substitutional elements, respectively [39–40]. Carbon enrichment in high-carbon retained austenite is a natural consequence of the bainitic transformation mechanism. However, the carbon concentration of austenite regions differs depending on the austenite morphology and thickness [41]. Austenite films can host much greater quantities of carbon than blocky austenites, which cause austenite blocks to be thermally less stable, especially at their center region.

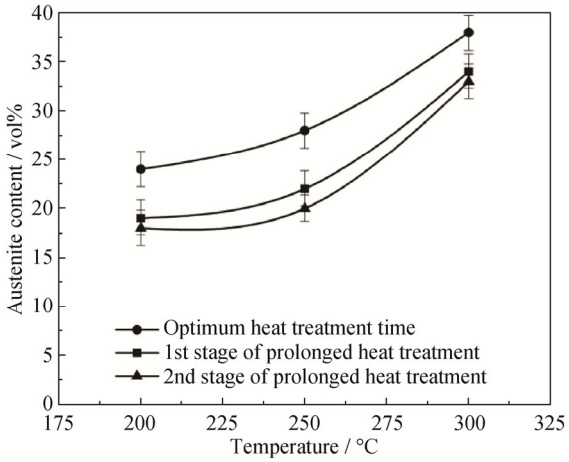

Fig. 2. Variations of the austenite volume fraction under optimum austempering conditions and after the first and second stages of prolonged isothermal heat treatments.

Table 2. Chemical composition of austenite under optimum austempering conditions and after the first and second stages of prolonged heat treatments

Alloying element content / wt%	Heat-treatment temperature and time								
	300°C			250°C			200°C		
	10 h	20 h	30 h	16 h	32 h	48 h	72 h	144 h	216 h
C	1.284	1.098	1.083	1.110	1.098	0.918	1.042	0.900	0.752
Si	1.613	1.616	1.617	1.616	1.616	1.619	1.617	1.620	1.622
Mn	1.195	1.197	1.198	1.197	1.197	1.200	1.198	1.202	1.202
Ni	2.540	2.544	2.545	2.544	2.544	2.549	2.546	2.549	2.553
Mo	0.269	0.269	0.269	0.269	0.269	0.270	0.270	0.270	0.270
Cr	0.996	0.998	0.998	0.998	0.998	1.000	0.998	1.000	1.001
V	0.100	0.100	0.100	0.100	0.100	0.100	0.100	0.100	0.100
Co	1.215	1.217	1.218	1.217	1.217	1.220	1.218	1.220	1.222
Al	0.886	0.888	0.882	0.888	0.888	0.890	0.889	0.890	0.891

A comparison of the carbon contents of retained austenites in Table 2 reveals that holding at the transformation time longer than necessary for completing the bainitic transformation led to a local reduction of the carbon content. This behavior can be explained by the fact that the microstructure was thermodynamically unstable and the high-carbon retained austenite attempted to slowly reach equilibrium by depletion of its excess carbon. Therefore, austenite lost its thermal stability and its volume fraction consequently decreased within the microstructure because austenite, which has a lower carbon content, was susceptible to transform to martensite during cooling to room temperature at the end of the prolonged stages of heat treatments.

Very detailed SEM studies revealed that the carbon rejected from the austenite phase precipitated as small particles within the microstructure at the end of the extended heat-treatment time even if the volume fraction of particles was relatively small. Examples of different precipitations in the sample austempered at 250°C for 48 h are shown in Figs. 3(a) and 3(b). Quantitative EDX analyses results, an example of which is given in Fig. 3(c) for a particular precipitate, show that the precipitates are enriched with iron and carbon. The relatively higher atomic percentages of iron and carbon in comparison with the other alloying elements in the EDX quantitative data indicate that the precipitates are likely cementite. The assignment of this phase as cementite becomes more reasonable when we consider that similar results have been reported for similar steels with similar microstructures [40], where detailed TEM observations revealed the presence of some cementite particle precipitations

with similar morphologies after prolonged austempering for 92 h at 200°C. However, precipitation contents in the aforementioned study were negligible and did not sufficiently impoverish the austenite phase to increase its martensite start temperature (M_s). Therefore, the volume fraction of austenite did not change, possibly because of the shorter extended time of bainitic reaction. However, longer prolonged heat-treatment time at transformation temperatures in the present study resulted in more severe carbon depletion from high-carbon retained austenite; therefore, the austenite lost its thermal stability to a greater extent, accompanied by its partial transformation to martensite during cooling to room temperature at the end of the first and second stages of the prolonged heat treatments. This partial transformation resulted in a decrease of the overall volume fraction of austenite in the final microstructure.

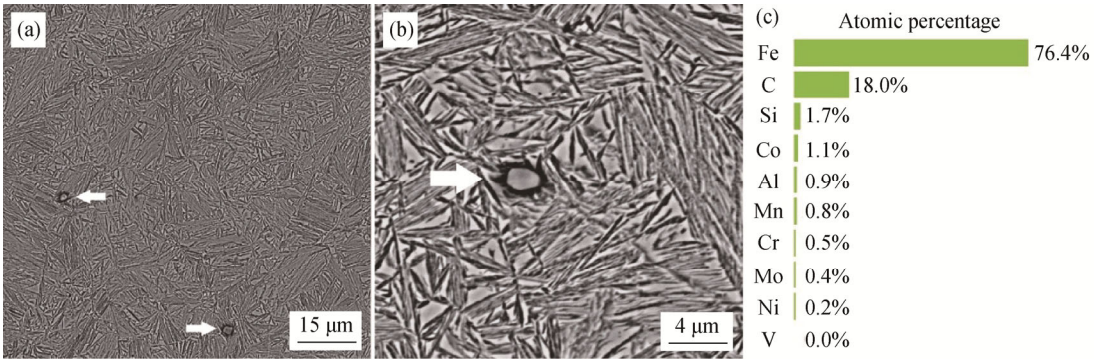

Fig. 3. Different precipitations in different locations of the sample austempered at 250°C for 48 h (a,b) and quantitative EDX analysis results for a particular precipitate within the microstructure at the end of the extended heat-treatment time (c).

Similar to a previous study [40], maintaining the steel for longer transformation time at each austempering temperature did not lead to the typical tempering sequence of a bainitic microstructure. This result means that no coarsening of bainitic subunits occurred and that austenite did not decompose into a mixture of ferrite and cementite layers (i.e., pearlite), which are expected to form at higher tempering temperatures, as previously reported [42]. Garcia-Mateo *et al.* [42] studied the tempering behavior of nanobainite obtained at 200°C at different temperatures ranging from 400 to 730°C, and they demonstrated that larger regions of retained austenite were susceptible to decomposition to pearlite at 550°C. Moreover, they have shown that prolonged tempering at 600°C resulted in microstructure coarsening. Therefore, we expected to find no traces of coarsening or decomposition because we carried out prolonged heat treatments at substantially lower temperatures.

3.2. Mechanical properties

We next investigated how the aforementioned microstructural evolutions affected the resultant mechanical properties. Mechanical properties of nanostructured advanced bainite are strongly dependent on the microstructural variations that occur during a prolonged isothermal heat treatment. The very high hardness value of advanced bainite is the direct consequence of nanoscale bainitic ferrites, and the expectation is to achieve higher hardness values when higher volume fractions of finer bainitic plates are achieved [43]. The high hardness value of advanced bainite is evident in Fig. 4, which shows the hardness variations at different stages of the bainitic heat treatment. The hardness of the material increased with decreasing transformation temperature at the end of the optimum heat-treatment times and also at the end of the prolonged heat-treatment stages. This behavior is due to the higher volume fractions of finer bainite formed within the microstructure at lower transformation temperatures. However, the results corresponding to prolonged heat-treatment conditions at a constant transformation temperature are misleading. The hardness values increased at longer transformation time despite the fact that the sizes of the bainitic ferrites were not affected by the extension of the transformation time beyond that needed for bainitic transformation to be completed. Therefore, microstructural sizes cannot solely describe the hardness enhancement with increasing heat-treatment time at each transformation temperature. The higher hardness values at longer transformation times are directly attributed to the presence of hard precipitates within the microstructure. These precipitates may also result in precipitation hardening, further increasing the hardness value even if their volume fraction is not considerable. Moreover, carbon rejection made the austenite phase being thermally less stable, resulting in its transformation into martensite. Thus, martensite formation was also responsible for increasing the hardness level under prolonged austempering heat-treatment conditions.

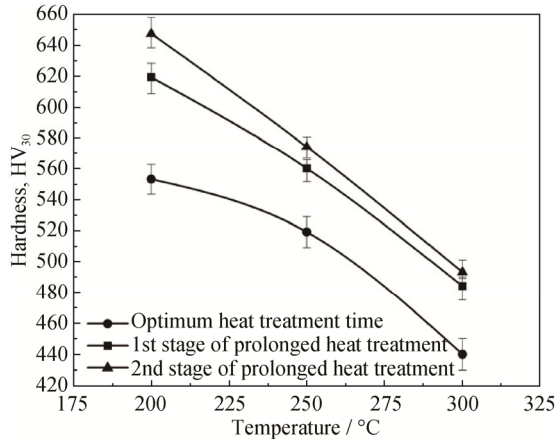

Fig. 4. Hardness variations in the optimum austempering conditions and after the first and second stages of prolonged heat treatments.

Microstructural changes also simultaneously affected the strength and ductility of the specimens. Fig. 5 shows examples of engineering stress–engineering strain curves obtained from tensile tests of the materials at room temperature. The curves show that extremely valuable strength and ductility combinations could be achieved at the end of the optimum heat treatment conditions. UTS values of 1600, 1890, and 2180 MPa were obtained along with 30%, 17%, and 14% total elongation at the end of the optimum heat-treatment times at 300, 250, and 200°C, respectively; much of the attained elongation was uniform. Moreover, continuous yielding also occurred during the tensile tests. This behavior is similar to that of strong dual-phase steels, which is related to the high density of free dislocations present within the microstructure; these dislocations were introduced during the shear transformation process of bainite [17].

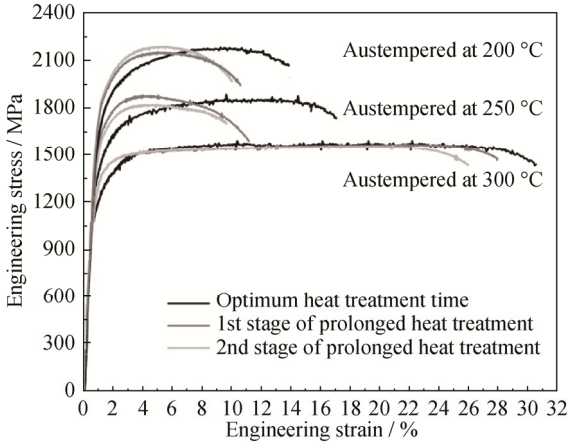

Fig. 5. Engineering stress–engineering strain curves under optimum austempering conditions and after the first and second stages of prolonged heat treatments.

Similar to the case of hardness variations, the volume fraction and the thickness of the bainitic subunits are the most important factors that must be considered when studying the strength properties. Higher volume fractions of finer bainitic ferrites increase the strength level, which is why higher UTS and higher yield strength (YS) values were achieved at lower transformation temperatures. Carbon in solid solution also substantially affects the strength properties. Bainitic ferrites are supersaturated with carbon, and higher densities of dislocations at the interface of bainitic subunits and the austenite phase prevent the carbon from partitioning toward austenite during bainite formation; this effect is more evident at lower transformation temperatures [22–24]. However, a large amount of carbon remains in solid solution in defect-free areas, which enhances the strength of the material through solid solution strengthening [17]. Notably, austenite also positively affects strength properties through the transformation-induced plasticity (TRIP) effect that occurs during tensile tests [17,33]. Austenite transforms into martensite when the sample is strained, and replacement of austenite by martensite increases the strength level considerably. Although the scale and the volume fraction of bainitic ferrites are the main factors affecting the strength properties, the amount of high-carbon retained austenite is the main factor influencing the ductility of the material. Higher volume fractions of austenite within the microstructure enable greater elongation levels at higher transformation temperatures at the end of the optimum heat-treatment time.

Having demonstrated the changes in strength and ductility properties at the end of the optimum heat-treatment stages, we next observed how prolonged austempering heat treatments affected the mechanical properties. Figs. 6 and 7 summarize the variations of the UTS, YS, and the total elongation with respect to the heat-treatment times at each transformation temperature, as determined from the results of tensile tests. Note that at least three tensile tests were conducted to ensure reproducibility of the variations. The results indicated that no relevant changes occurred in the UTS values when the heat-treatment time at each austempering temperature was extended. Nevertheless, increasing the isothermal heat treatment time enhanced the YS and decreased the total elongation levels even if the changes from the first to the second stage of the prolonged heat treatment were not substantial. Almost constant UTS values at different heat-treatment stages can be explained by the fact that the volume fraction and thicknesses of the extremely fine bainitic ferrites were almost identical at any stage of heat treatment at a constant transformation temperature. Although the

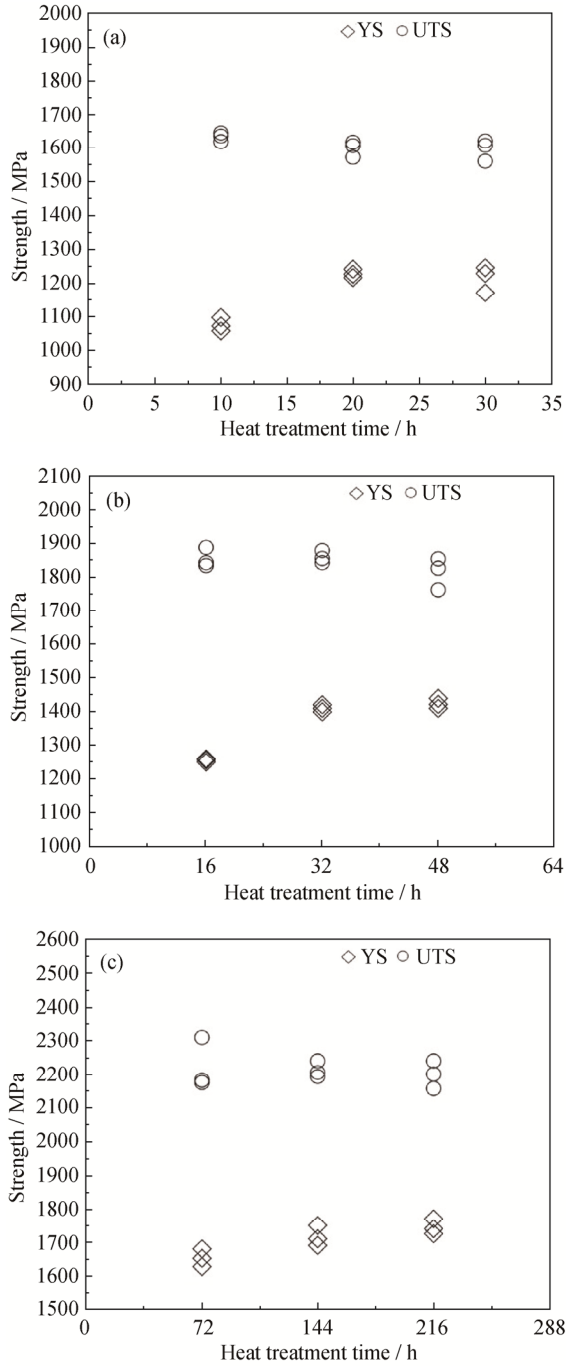

Fig. 6. Variations of UTS and YS under the optimum austempering conditions and after the first and second stages of prolonged heat treatments at 300°C (a), 250°C (b), and 200°C (c).

precipitates were expected to improve the UTS values, their effect was diminished because of their small number. However, the effect of the precipitates was at least adequate to increase the YS to some extent despite their low volume fraction because they pinned the free dislocations, thereby restricting dislocation glides. Previous studies [17] have shown that strain accommodation in austenite during the shear transformation of bainite results in dislocation densities of almost 5×10^{15} m^{-2} in austenite in similar steels austempered at 300°C, where the dislocation densities increase with decreasing transformation temperature. Moreover, as previously demonstrated, carbide precipitations at prolonged austempering stages in this study decreased the amount of carbon of retained austenite, which made this phase thermally less stable and caused austenite to partially transform into martensite during cooling to room temperature. Martensite formation accompanies the introduction of extra dislocations into the microstructure, which adds up to the pre-existing dislocation density present within the microstructure of bainitic steel as a result of the shear mechanism of the bainitic reaction. Thus, the presence of martensite, the introduction of higher dislocation densities into the microstructure, hard carbide precipitations, and dislocation pinning by precipitates increased the YS of the material under prolonged isothermal heat-treatment conditions.

Lower volume fractions of high-carbon retained austenites after prolonged austempering heat treatments were responsible for lower elongation values because the austenite phase is the main factor controlling the ductility of the nanostructured advanced bainitic steels. Additionally, carbide precipitations further deteriorated the ductility. Irrespective of the amount of austenite, its mechanical stability also adversely affects the elongation value [16,44]. Mechanically less stable austenite converts into martensite during the early stages of the tensile tests; therefore, austenite cannot play an effective role in ductility enhancement. On the other hand, if austenite becomes mechanically too stable, the TRIP effect cannot be effective. Therefore, a moderate mechanical stability of austenite is necessary to enhance the strength and ductility combination in nanostructured bainite [33,45]. Considering that the amount of carbon is the strongest parameter affecting the mechanical stability of retained austenite, decreasing the carbon in solid solution in austenite during the first and second stages of prolonged heat treatments reduced its mechanical stability and further reduced the total elongation.

Fig. 8 represents the variation in impact toughness energy with respect to heat-treatment temperature at the optimum and prolonged austempering stages. Increasing the transformation temperature from 200 to 250°C enhanced the values of impact energy absorption, although it decreased again at 300°C irrespective of the transformation time. In addition, prolonged austempering heat treatments deteriorated the toughness property at all transformation temperatures. Various parameters affect the toughness properties of advanced bainite; however, variations in the volume fraction

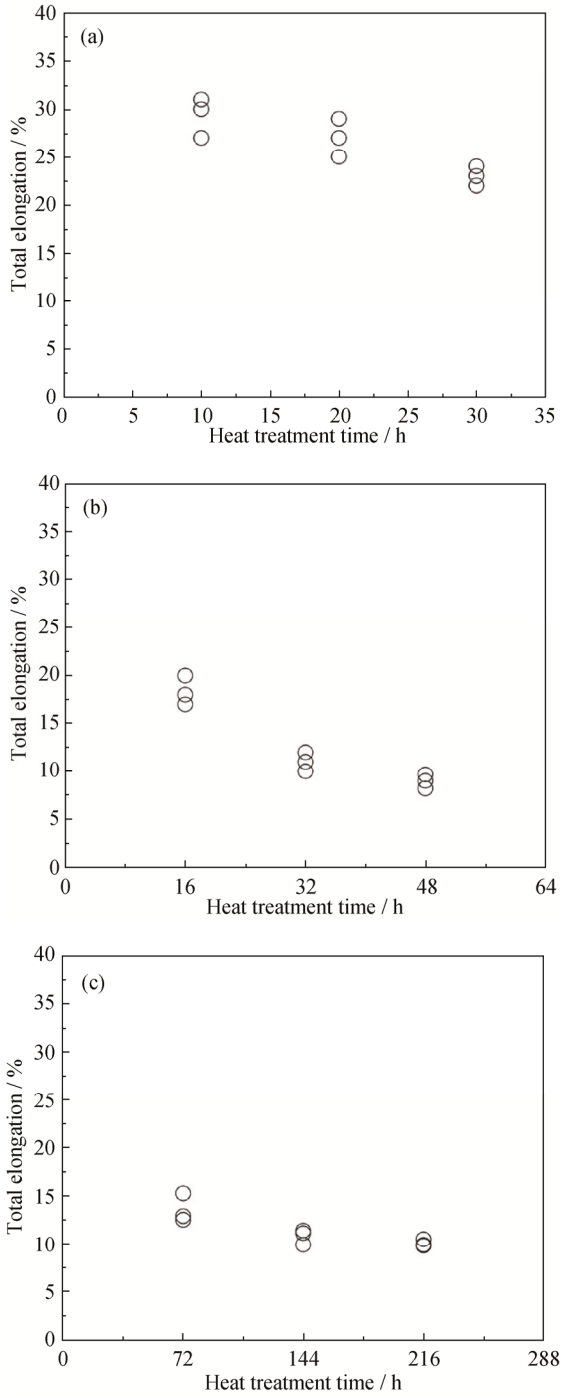

Fig. 7. Variations of total elongation under the optimum austempering conditions and after the first and second stages of prolonged heat treatments at 300°C (a), 250°C (b), and 200°C (c).

of high-carbon retained austenite and its morphology are the most critical factors that must be taken into account [46–48]. Additionally, in the present study, a low volume fraction, size, and distribution of precipitations played a role in determining the impact toughness during the charpy impact test in samples isothermally heat treated for prolonged heat-treatment times. Ductile austenite plays a critical role in controlling the impact toughness of advanced bainite through the blunting of crack tips, thereby restricting its growth and propagation. Regardless of the heat-treatment temperature, decreasing the austenite content, increased martensite formation, and increased carbide precipitations at prolonged heat-treatment stages all deteriorated the impact toughness of materials, even if determining which of the aforementioned factors had the strongest effect is difficult. In addition, carbide precipitation and carbon rejection from austenite during the prolonged heat treatment decreased the mechanical stability of austenite and made this phase ineffective in crack blunting through early transformation to brittle martensite during straining.

Notably, the volume fraction of austenite cannot solely control the impact energy absorption because, if the austenite content is the only governing parameter, then the value of the impact energy would be greater at 300°C because of the higher volume fraction of this phase within the microstructure. Thus, the morphology of the retained austenite should also be considered, as suggested in a previous work [48]. Higher volume fractions of austenite blocks were present at 300°C, which is why the value of the impact energy was lower than that at 250°C. A greater amount of bainite formed at 250°C, which resulted in increased consumption of primary austenite and, consequently, a lower volume fraction; finer austenite blocks could be achieved within the microstructure. Therefore, the material exhibited lower impact toughness values contrary to its higher volume fraction of austenite at 300°C at all transformation times investigated in this study. Austenite blocks are thermally and mechanically less stable and transform quickly into martensite during the impact test. Therefore, austenite cannot play its beneficial role in blunting the cracks and enhancing the impact toughness of the material.

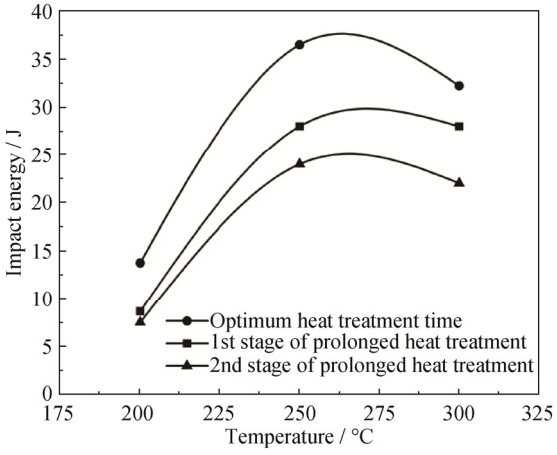

Fig. 8. Impact energy observed after austempering under optimum conditions and after the first and second stages of prolonged heat treatments.

4. Conclusions

(1) The sizes of microstructural constituents were completely unaffected by prolonged heat-treatment times, and the microstructural constituents with approximate thicknesses of 41–88 nm could be achieved.

(2) Although 38vol%, 28vol%, and 24vol% of high-carbon retained austenite were present within the microstructure when bainitic transformation was completed at 300, 250, and 200°C, respectively, it decreased to almost 34vol%, 22vol%, and 19vol% at the end of the first stage and 33vol%, 20vol%, and 18vol% at the end of the second stage of the prolonged heat treatment times. This has been rationalized on the basis of carbon depletion from high-carbon retained austenite, which caused the austenite phase to lose its thermal stability and consequently transform into martensite during cooling to room temperature.

(3) Prolonged austempering resulted in some precipitations. Martensite formation and precipitations within the microstructure both increased the hardness values at extended heat-treatment times. Although the UTS values were kept almost constant by extending the heat-treatment time beyond the optimum criterion at a constant transformation temperature, microstructural evolutions increased the YS of the materials.

(4) Prolonged heat treatments were observed to decrease both the total elongation and the impact toughness values even if an acceptable balance of strength and ductility were still achieved.

Acknowledgments

The author is grateful to Azarbaijan Shahid Madani University for providing the research facilities.

References

[1] H.K.D.H. Bhadeshia and D.V. Edmonds, Bainite in silicon steels: new composition-property approach Part 1, *Met. Sci.*, 17(1983), p. 411.

[2] H.K.D.H. Bhadeshia and D.V. Edmonds, Bainite in silicon steels: new composition-property approach Part 2, *Met. Sci.*, 17(1983), p. 420.

[3] S. Khare, K. Lee, and H.K.D.H. Bhadeshia, Carbide-free bainite: compromise between rate of transformation and properties, *Metall. Mater. Trans. A*, 41(2010), No. 4, p. 922.

[4] F.G. Caballero, H.K.D.H. Bhadeshia, K.J.A. Mawella, D.G. Jones, and P. Brown, Very strong low temperature bainite, *Mater. Sci. Technol.*, 18(2002), p. 279.

[5] F.G. Caballero and H.K.D.H. Bhadeshia, Very strong bainite, *Curr. Opin. Solid State Mater. Sci.*, 8(2004), No. 3-4, p. 251.

[6] C. García Mateo, F.G. Caballero, and H.K.D.H. Bhadeshia, Development of hard bainite, *ISIJ Int.*, 43(2003), No. 8, p. 1238.

[7] M.N. Yoozbashi and S. Yazdani, Mechanical properties of nanostructured, low temperature bainitic steel designed using a thermodynamic model, *Mater. Sci. Eng. A*, 527(2010), No. 13-14, p. 3200.

[8] M.N. Yoozbashi, S. Yazdani, and T.S. Wang, Design of a new nanostructured, high-Si bainitic steel with lower cost production, *Mater. Des.*, 32(2011), No. 6, p. 3248.

[9] C. Garcia-Mateo and F.G. Caballero, Design of carbide-free low-temperature ultra high strength bainitic steels, *Int. J. Mater. Res.*, 98(2007), No. 2, p. 137.

[10] C. Garcia-Mateo and F.G. Caballero, Ultra-high-strength bainitic steels, *ISIJ Int.*, 45(2005), No. 11, p. 1736.

[11] H.K.D.H. Bhadeshia, Nanostructured bainite, *Proc. R. Soc. A*, 466(2010), p. 3.

[12] F.G. Caballero, M.J. Santofimia, C. Capdevila, C. García-Mateo, and C. García de Andrés, Design of advanced bainitic steels by optimisation of TTT diagrams and T0 curves, *ISIJ Int.*, 46(2006), No. 10, p. 1479.

[13] F.G. Caballero, M.J. Santofimia, C. García-Mateo, J. Chao, and C.G. de Andrés, Theoretical design and advanced microstructure in super high strength steels, *Mater. Des.*, 30(2009), No. 6, p. 2077.

[14] C. Garcia-Mateo, F.G. Caballero, T. Sourmail, J. Cornide, V. Smanio, and R. Elvira, Composition design of nanocrystalline bainitic steels by diffusionless solid reaction, *Met. Mater. Int.*, 3(2014), No. 3, p. 405.

[15] Y. Huang, A.M. Zhao, J.G. He, X.P. Wang, Z.G. Wang, and L. Qi, Microstructure, crystallography and nucleation mechanism of NANOBAIN steel, *Int. J. Miner. Metall. Mater.*, 20(2013), No. 12, p. 1155.

[16] C. Garcia-Mateo, F.G. Caballero, T. Sourmail, M. Kuntz, J. Cornide, V. Smanio, and R. Elvira, Tensile behaviour of a nanocrystalline bainitic steel containing 3wt% silicon, *Mater. Sci. Eng. A*, 549(2012), p. 185.

[17] B. Avishan, S. Yazdani, F.G. Caballero, T.S. Wang, and C. Garcia-Mateo, Characterisation of microstructure and mechanical properties in two different nanostructured bainitic steels, *J. Mater. Sci. Technol.*, 31(2015), No. 12, p. 1508.

[18] H.K.D.H. Bhadeshia, *Bainite in Steels,* 2nd Ed., Institute of Materials, London, 2001, p. 117.

[19] F.G. Caballero, M.K. Miller, C. Garcia-Mateo, and J. Cornide, New experimental evidence of the diffusionless transformation nature of bainite, *J. Alloys Compd.*, 577(2013), No. s1, p. 626.

[20] H. Bhadeshia and J. Christian, Bainite in steels, *Metall. Trans. A*, 21(1990), No. 3, p. 767.

[21] F.G. Caballero, M.K. Miller, and C. Garcia-Mateo, The approach to equilibrium during tempering of a bulk nanocrystalline steel: an atom probe investigation, *J.* Mater. *Sci.*,

43(2008), No. 11, p. 3769.

[22] F.G. Caballero, M.K. Miller, S.S. Babu, and C. García-Mateo, Atomic scale observations of bainite transformation in a high carbon high silicon steel, *Acta Mater.*, 55(2007), No. 1, p. 381.

[23] J. Cornide, G. Miyamoto, F.G. Caballero, T. Furuhara, M.K. Miller, and C. García-Mateo, Distribution of dislocations in nanostructured bainite, *Solid State Phenom.*, 172-174(2011), p. 117.

[24] F.G. Caballero, H.W. Yen, M.K. Miller, J.R. Yang, J. Cornide, and C. Garcia-Mateo, Complementary use of transmission electron microscopy and atom probe tomography for the examination of plastic accommodation in nanocrystalline bainitic steels, *Acta Mater.*, 59(2011), No. 15, p. 6117.

[25] H.K.D.H. Bhadeshia and A.R. Waugh, Bainite: An atom-probe study of the incomplete reaction phenomenon, *Acta Metall.*, 30(1982), No. 4, p. 775.

[26] F.G. Caballero, C. Garcia-Mateo, M.J. Santofimia, M.K. Miller, and C. García de Andrés, New experimental evidence on the incomplete transformation phenomenon in steel, *Acta Mater.*, 57(2009), No. 1, p. 8.

[27] M. Kabirmohammadi, B. Avishan, and S. Yazdani, transformation kinetics and microstructural features in low-temperature bainite after ausforming process, *Mater. Chem. Phys.*, 184(2016), p. 306.

[28] H.K.D.H. Bhadeshia and D.V. Edmonds, The bainite transformation in a silicon steel, *Metall. Trans. A*, 10(1979), No. 7, p. 895.

[29] A. Saha Podder and H.K.D.H. Bhadeshia, Thermal stability of austenite retained in bainitic steels, *Mater. Sci. Eng. A*, 527(2010), No. 7-8, p. 2121.

[30] F.G. Caballero, H.K.D.H. Bhadeshia, K.J.A. Mawella, D.G. Jones, and P. Brown, Design of novel high strength bainitic steels: Part 2, *Mater. Sci. Technol.*, 17(2001), No. 5, p. 517.

[31] H.S. Hasan, M.J. Peet, and H.K.D.H. Bhadeshia, Severe tempering of bainite generated at low transformation temperatures, *Int. J. Mater. Res.*, 103(2012), No. 11, p. 1319.

[32] C. García-Mateo, F.G. Caballero, and H.K.D.H. Bhadeshia, Acceleration of low-temperature bainite, *ISIJ Int.*, 43(2003), No. 11, p. 1821.

[33] B. Avishan, C. Garcia-Mateo, L. Morales-Rivas, S. Yazdani, and F.G. Caballero, Strengthening and mechanical stability mechanisms in nanostructured bainite, *J. Mater. Sci.*, 48(2013), p. 6121.

[34] L.C. Chang and H.K.D.H. Bhadeshia, Austenite films in bainitic microstructures, *Mater. Sci. Technol.*, 11(1995), p. 874.

[35] B.D. Cullity and S.R. Stock, *Elements of X-ray Diffraction,* 3rd Ed., PrenticeHall, New York, 2001.

[36] D.J. Dyson and B. Holmes, Effect of alloying additions on the lattice parameter of austenite, *J. Iron Steel Inst*., 208(1970), No. 5, p. 469.

[37] H.W. King and E.A. Payzant, Error corrections for X-ray powder diffractometry, *Can. Metall. Q.*, 40(2001), No. 3, p. 385.

[38] S.B. Singh and H.K.D.H. Bhadeshia, Estimation of bainite plate-thickness in low-alloy steels, *Mater. Sci. Eng. A*, 245(1998), No. 1, p. 72.

[39] F.G. Caballero, M.K. Miller, and C. Garcia-Mateo, Tracking solute atoms during bainite reaction in a nanocrystalline steel, *Mater. Sci. Technol.*, 26(2010), No. 8, p. 889.

[40] B. Avishan, C. Garcia-Mateo, S. Yazdani, and F.G. Caballero, Retained austenite thermal stability in a nanostructured bainitic steel, *Mater. Charact.*, 81(2013), p. 105.

[41] C. Garcia-Mateo, F.G. Caballero, M.K. Miller, and J.A. Jimenez, On measurement of carbon content in retained austenite in a nanostructured bainitic steel, *J. Mater. Sci.*, 47(2012), No. 2, p. 1004.

[42] C. Garcia-Mateo, M. Peet, F.G. Caballero, and H.K.D.H. Bhadeshia, Tempering of hard mixture of bainitic ferrite and austenite, *Mater. Sci. Technol.*, 20(2004), No. 7, p. 814.

[43] C. Garcia-Mateo, F.G. Caballero, and H.K.D.H. Bhadeshia, Low temperature bainite, *J. Phys. IV*, 112(2003), p. 285.

[44] C. Garcia-Mateo, F.G. Caballero, J. Chao, C. Capdevila, and C.G. de Andres, Mechanical stability of retained austenite during plastic deformation of super high strength carbide free bainitic steels, *J. Mater. Sci.*, 44(2009), No. 17, p. 4617.

[45] A. Kammouni, W. Saikaly, M. Dumont, C. Marteau, X. Bano, and A. Charaï, Effect of the bainitic transformation temperature on retained austenite fraction and stability in Ti microalloyed TRIP steels, *Mater. Sci. Eng. A*, 518(2009), No. 1-2, p. 89.

[46] F.G. Caballero, J. Chao, J. Cornide, C. García-Mateo, M.J. Santofimia, and C. Capdevila, Toughness deterioration in advanced high strength bainitic steels, *Mater. Sci. Eng. A*, 525 (2009), p. 87.

[47] S. Golchin, B. Avishan, and S. Yazdani, Effect of 10% ausforming on impact toughness of nano bainite austempered at 300°C, *Mater. Sci. Eng. A*, 656 (2016), p. 94.

[48] B. Avishan, S. Yazdani and S.H. Nedjad, Toughness variations in nanostructured bainitic steels, *Mater. Sci. Eng. A*, 548(2012), p. 106.